Geophysical Research Letters

RESEARCH LETTER
10.1029/2023GL104311

Key Points:

- Near-full-depth Conductivity-Temperature-Depth (CTD) casts data collected in the Ionian Sea with an unorthodox methodology allowed resolving tidal scale
- The temperature and salinity diagram depicted typical water masses for the Ionian area including a dense abyssal water mass
- The analyses showed a periodic pulsation and an activation of mixing in the abyssal layer due to the baroclinic internal tide

Correspondence to:
N. Lo Bue,
nadia.lobue@ingv.it

Citation:
Giambenedetti, B., Lo Bue, N., Kokoszka, F., Artale, V., & Falcini, F. (2023). Multi-approach analysis of baroclinic internal tide perturbation in the Ionian Sea abyssal layer (Mediterranean Sea). *Geophysical Research Letters*, *50*, e2023GL104311. https://doi.org/10.1029/2023GL104311

Received 28 APR 2023
Accepted 30 JUN 2023

Multi-Approach Analysis of Baroclinic Internal Tide Perturbation in the Ionian Sea Abyssal Layer (Mediterranean Sea)

B. Giambenedetti[1,2], N. Lo Bue[2], F. Kokoszka[3], V. Artale[2,4], and F. Falcini[4]

[1]Department of Physics, University of Rome Tor Vergata, Rome, Italy, [2]Istituto Nazionale di Geofisica e Vulcanologia (INGV), Rome, Italy, [3]Stazione Zoologica Anton Dohrn, Napoli, Italy, [4]National Research Council (CNR), Institute of Marine Sciences (ISMAR), Rome, Italy

Abstract Despite being widely recognized, the importance of deep layers thermohaline and mixing processes in the ocean circulation and variability is still poorly investigated, especially in the Mediterranean Sea. This limits understanding and parametrizing deep dynamics, which result in evident biases in the global circulation representation by observations and numerical ocean simulations. Having access to hydrological datasets, collected on a whole water column, we investigated the abyssal stratification and its variability of the Ionian Sea (Central Mediterranean). Applying multiple analyses, we found a tidal-period oscillation and the resulting activation of mixing, pointing out that the combined effect of stratification, morphology, and tides has a key role in enhancing local diapycnal diffusivity in the deepest layers, being a mechanism that connects the whole water column with a compelling impact on the vertical transport of heat and tracers.

Plain Language Summary The presence of a quasi-homogeneous density layer in the deep sea made it possible to observe a periodic effect: the layer acts like a "cushion" that is pulled up and then readjusted in circa 12 hr, which is the period typical of tides. The fact that tides can propagate down to the sea interior impacting the deep processes, down to 3,000 m of depth, is not so straightforward to observe. The deep ocean has a very slow dynamic, and the physical-chemical phenomena involved are still mostly unknown.

1. Introduction

The processes and the dynamics in the deep sea are still not fully understood, due to system complexity and lack of observation (Fox-Kemper, 2021; Glover et al., 2010; Ruhl et al., 2011; Stammer et al., 2018). In particular, below 2,000 m of depth, there is a scarcity of full-depth observations of the water column and long-time deep data sets, and this also applies in the Mediterranean Sea (Artale et al., 2018; Tintoré et al., 2019). Given the paucity of data, the high cost of deep-sea monitoring, and the sustainability issue of such exploration, it is important to integrate all available resources trying to get as much information as possible from data collected over time, exploiting different methodologies to answer the open questions on the deep-sea dynamics (Levin et al., 2019; Nash et al., 2022; Polejack, 2021).

The upper ocean is dominated by its stable stratification, being directly heated from above by solar radiation. The abyssal stratification is not as easily explained since there is no primary heat source and other processes govern it. For instance, estimates of heat storage in the deep layer of the Ionian abyssal plain were equivalent of ~1.62 W/m^2 (Artale et al., 2018), more than double the global mean anomaly due to climate change. In this area, the geothermal heat fluxes at the seafloor are too weak to explain such heat buildup (Makris & Stobbe, 1984). This accumulation of energy is connected to the Eastern Mediterranean Transient, the major climate event that affected the eastern Mediterranean at the end of the eighties and culminated in the nineties (Artale et al., 2018; Bensi et al., 2016; Hainbucher et al., 2006; Incarbona et al., 2016; Klein et al., 1999; P. Li & Tanhua, 2020; Manca, 2003; Manca et al., 2006; Roether et al., 1996; Theocharis et al., 2002). Nonetheless, it is well established that the energy stored in the abyss can be reintroduced into circulation and redistributed by local processes (Ferrari et al., 2016). This is likely to have an impact on the decadal climatic variability of the Mediterranean Sea, with the tides playing a significant role (Artale et al., 2018; van Haren & Gostiaux, 2011).

Small-scale mixing generated by internal wave breaking is not enough to explain the energy budget (Klocker & McDougall, 2010; Kunze et al., 2012; Polzin et al., 1997; Simmons et al., 2004). It has been pointed to the

crucial role of currents and mixing in the turbulent boundary layers over sloping rough bathymetry as well as the interaction with the inertial band of the internal wave spectrum in the abyssal circulation (De Lavergne et al., 2022; Ferrari et al., 2016; Rubino et al., 2007; St. Laurent et al., 2001; Wunsch & Ferrari, 2004). The baroclinic tidal component has been recognized in the ocean as the most eligible process to drive and explain deep circulation, enhancing abyssal mixing (MacKinnon et al., 2017; St. Laurent et al., 2001; Wüest & Lorke, 2003; Wunsch & Ferrari, 2004). These effects on the ocean interior and their consequences on the circulation have yet to be sufficiently investigated, especially in the Mediterranean basin, due to the area's limited amplitude of the tides (Cushman-Roisin & Naimie, 2002; Millot & Taupier-Letage, 2005). The tidal effects in this basin show an evident example in the Messina Strait, where they generate internal solitary waves propagating at ∼1 m/s observed both by in situ observations and by remote sensing (Artale et al., 1990; Cavaliere et al., 2021). Moreover, numerical model simulations with explicit tidal forcing demonstrated that tides have a non-negligible effect on intermediate circulation and in deep water convection processes, but less evidence on the abyssal layer, both in the global ocean (Arbic, 2022; Arbic et al., 2018; Z. Li et al., 2015; Müller et al., 2012; Waterhouse et al., 2014) and in the Mediterranean region (Sannino et al., 2015, 2022; Tsimplis et al., 1995).

The horizontal and vertical circulations in the Ionian Sea are driven by the combined effect of wind stress and thermohaline components, are strongly affected by the basin geometry, and are characterized by sub-mesoscale gyres and variable currents (Pinardi et al., 2015; Robinson et al., 1991). During summer, the Modified Atlantic Water (MAW), which spreads eastward from the Sicily Strait in the surface layer, is well-defined and distinct from the warmer and saltier Ionian surface water, while they are mixed throughout the rest of the year. The MAW overlies the Levantine Intermediate Water (LIW) in the layer between 200 and 800 m, while the abyssal layers of the Ionian Sea are usually occupied by the Eastern Mediterranean Deep Water (EMDW), which originates from the mixing of Atlantic Deep Water and deep waters of Adriatic origin (Astraldi et al., 2002; Bensi et al., 2013; Budillon et al., 2010; Pinardi et al., 2015; Theocharis et al., 1993; Wüst, 1961).

In this letter, we investigate how tidal forcing influences diffusion in the deepest layers in the Ionian Sea. Our analysis is based on the unusual approach used in performing Conductivity-Temperature-Depth (CTD) casts, consisting of recurring full-depth profiles with a short time lag, which are unusually taken on hydrological cruises, mostly because of time-demanding operations and the need of monitoring larger areas. We combined this data set with a normal mode decomposition analysis, which has been widely used for studying internal waves in the ocean (Cao et al., 2015; Garrett & Munk, 1979; Gill, 1982; Griffiths & Grimshaw, 2007; Pauthenet et al., 2019), but rarely for deep-sea analysis (Alford, 2003; Artale et al., 2018), and estimates of the diapycnal diffusivity. Even though they have never been considered sufficient to resolve this type of dynamics, here we explore repeated CTD profiles finding comforting results and shedding light on abyssal mixing processes.

2. Data and Methods

2.1. CTD Data

The data we use in this work refer to near-full-depth CTD profiles carried out in the Ionian abyssal plain of the Eastern Mediterranean Sea at about 70 km from the Malta Escarpment, at the ER-0121 site (36° 18′ N, 16° 6′ E), from 1999 to 2003 (see Figure 1; Table 1). The temperature and salinity profiles (Figure 2) used have been post-processed following the common quality control standards and the Intergovernmental Oceanographic Commission (IOC) recommendations (Bushnell et al., 2019; IOC et al., 2010).

2.2. Normal Mode Decomposition in Q-G Approximation

To study the oscillations of the water column we performed a normal mode decomposition on the assumption of Quasi-Geostrophic (Q-G) dynamics on the vertical profiles of buoyancy frequency (N^2), which was calculated directly from in-situ data. Modal shapes depend strongly on the amount of filtering applied to the profile. We obtained the best performances for real data input with a Savinsky-Golay filter of order 1 and frame length 15. The Q-G equation in a continuously stratified fluid on a beta plane is (Gill, 1982; Pedlosky, 1996):

$$\begin{cases} \dfrac{\partial q}{\partial t} = 0 \\ q = \nabla^2 p + \rho \dfrac{\partial}{\partial z}\left(\dfrac{1}{\rho N^2}\dfrac{\partial p}{\partial z}\right) + \beta_0 \dfrac{\partial p}{\partial x} \end{cases} \tag{1}$$

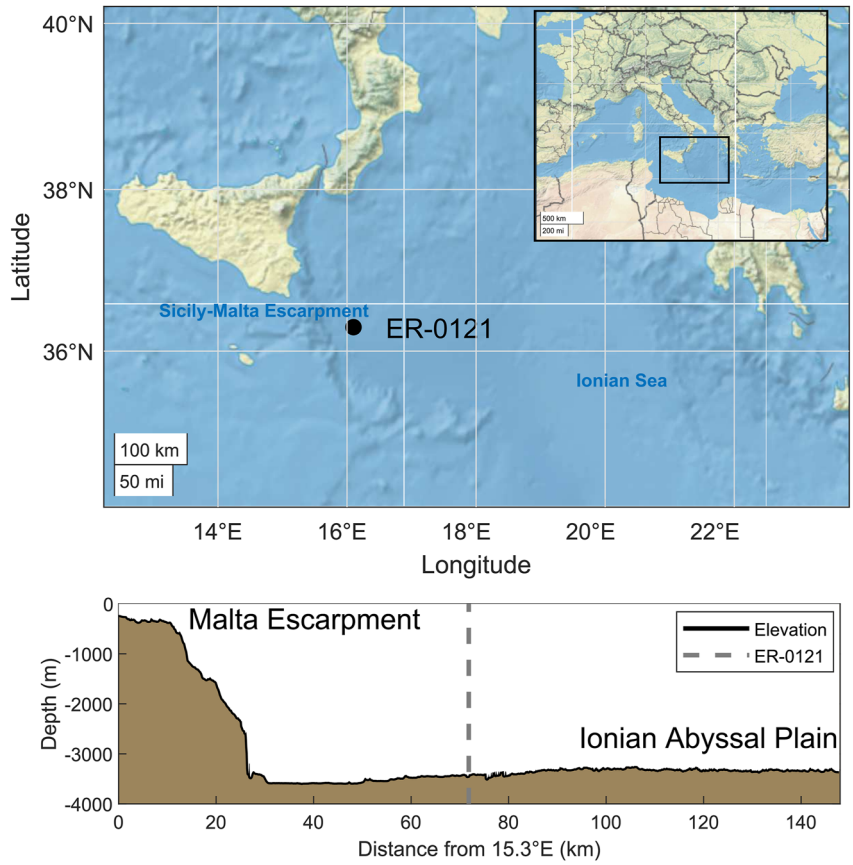

Figure 1. Bathymetric map of the Ionian Sea indicating the location of the Conductivity-Temperature-Depth station (ER-0121). The bottom panel shows details of the bathymetric profile (data from EMODNET Bathymetry DTM 2020, https://emodnet.ec.europa.eu/en/bathymetry).

where q is the potential vorticity, p is pressure, ρ is density, and the Coriolis parameter is $f = f_0 + \beta_0 y$, with $|\beta_0 y| \ll f_0$. By assuming a solution of the form: $p(x, y, z, t) = \tilde{p}(z)e^{i(k_x x + k_y y - \omega t)}$, substitution in Equation 1 yields to a Sturm-Liouville (S-L) problem:

$$\rho \frac{d}{dz}\left(\frac{1}{\rho N^2}\frac{d\tilde{p}}{dz}\right) + \frac{1}{gh_n}\tilde{p} = 0 \tag{2}$$

where the separation constant is: $gh_n = \frac{1}{\left(\frac{\beta_0 k_x}{\omega} + k_x^2 + k_y^2\right)}$.

To solve the S-L problem we assumed that the fluid is bounded below by a horizontal surface, and above by a free surface. Together with its boundary conditions, the S-L equation defines an eigenvalue problem where the eigenvalues are determined by the vertical profiles of N^2, and the eigenvectors are the vertical modes corresponding to each eigenvalue. The discretization used here was a straightforward finite-difference technique, with uniform spacing between vertical levels of ~10 m.

The resulting baroclinic modes from the solution of Equation 2 are the internal modes of oscillation associated with the vertical changes in the stratification. The zero-crossing intercepts the layer oscillation (Figure 3): each mode behaves as a step change moving out from the initial discontinuity. The first baroclinic mode, which is the most energetic, represents the oscillatory behavior due to the strong maximum of N^2 that is often found near the ocean surface, since generally the first 200 m are the most stratified (LeBlond & Mysak, 1978). The next vertical shapes of the modes are the different ranges of the scale of the stratification variability, and the fifth mode is the first able to capture the baroclinic structure of the deepest layer (Artale et al., 2018).

Table 1
Summary of the Conductivity-Temperature-Depth Casts Used in This Work, Performed at the ER-0121 Location

Cast name	Date (dd mm yyyy)	Cast start time (hh:mm:ss)	Depth range (m)
M08 CTD 02	18 December 1999	22:35:13	205–3,270
M08 CTD 06	19 December 1999	10:14:31	
M08 CTD 10	19 December 1999	22:59:06	
M17 CTD 07	13 March 2002	23:26:34	52–3,009
M17 CTD 11	14 March 2002	14:48:56	
M17 CTD 14	15 March 2002	10:34:52	
M17 CTD 17	15 March 2002	21:28:34	
M18 CTD 04	30 April 2002	06:42:18	51–3,000
M18 CTD 09	30 April 2002	13:43:16	
M18 CTD 13	30 April 2002	16:42:56	
M20 CTD 21	14 August 2002	00:53:45	194–3,256
M20 CTD 26	14 August 2002	20:26:10	
M20 CTD 30	16 August 2002	10:36:05	
M22 CTD 13	22 July 2003	10:13:00	97–3,235
M22 CTD 18	22 July 2003	22:05:28	

2.3. Diffusivity Estimation Method

The vertical eddy diffusivity coefficient is generally estimated and parametrized from CTD and velocity measurements since there are few direct observations and microstructure profiler measurements have many underlying difficulties (Nakano & Yoshida, 2019). The most physically consistent and well-established methodology to give estimates of the coefficient (Osborn, 1980; Osborn & Cox, 1972; Toole et al., 1994), is the Osborn relation under steady-state condition in a conventional turbulence system: $K = \Gamma \epsilon N^{-2}$ where ϵ is dissipation rate of turbulent kinetic energy, and the mixing efficiency Γ is taken constant (Koseff et al., 2016; Kunze et al., 2006; Oakey, 1982; Osborn, 1980). This equation allows estimating vertical diffusivity directly from dissipation rate and buoyancy. Most of the mixing is bounded to the internal wave field, so that is possible to express the dissipation rate as the anomaly of the strain variances from the background state of the internal wave field represented by the Garrett and Munk (hereafter GM) model (Artale et al., 2018; Gregg et al., 2003; Kunze et al., 2006):

$$K_{iw} = K_0 \frac{<\xi_z^2>^2}{<\xi_z^2>_{GM}^2} F_2(R_\omega)\lambda(f, N) \tag{3}$$

where $F_2(R_\omega) = \frac{1}{6\sqrt{2}} \frac{R_\omega(R_\omega+1)}{\sqrt{R_\omega - 1}}$ and $R_\omega = 7$ (3 for the GM spectrum), $\lambda\left(\frac{f}{N}\right) = \frac{f \cosh^{-1}(N/f)}{f_0 \cosh^{-1}(N_0/f_0)}$ is the latitude dependence, and $K_0 = 0.05 \cdot 10^{-4}$ m^2/s.

The internal wave strain can be estimated directly from N^2, following the strain-based parametrization (Artale et al., 2018; Kunze et al., 2006):

$$\xi_Z = \frac{N^2 - \overline{N^2}}{\overline{N^2}} \tag{4}$$

where $\overline{N^2}$ is the mean profile, in our case the time average. The ξ_Z of each z-segment have been windowed at both ends with a 10% Tukey windowing before transforming to obtain strain spectrum, from which the strain

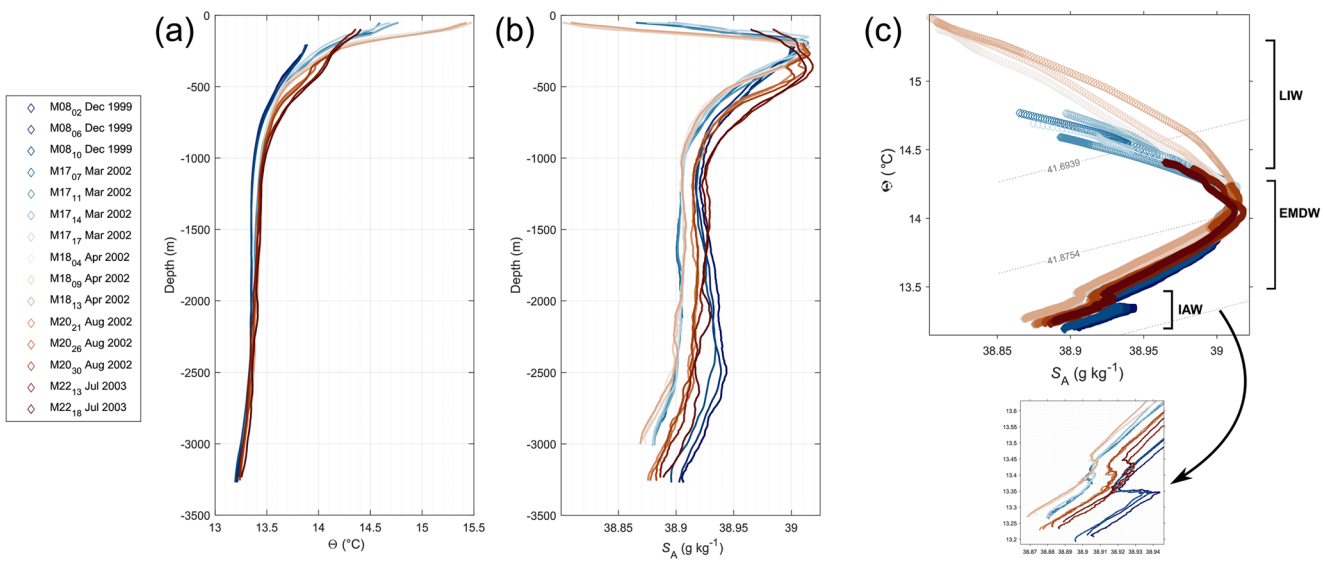

Figure 2. Measured (a) conservative temperature (Θ) and (b) absolute salinity (S_A) profiles; (c) $S_A - \Theta$ diagram. Water masses are indicated by their acronym. On the left, color legend according to the names and periods of the casts. On the bottom right side of the panel a zoom of the deepest zone corresponding to the Ionian Abyssal Water. Colormap by Crameri (Crameri, 2018).

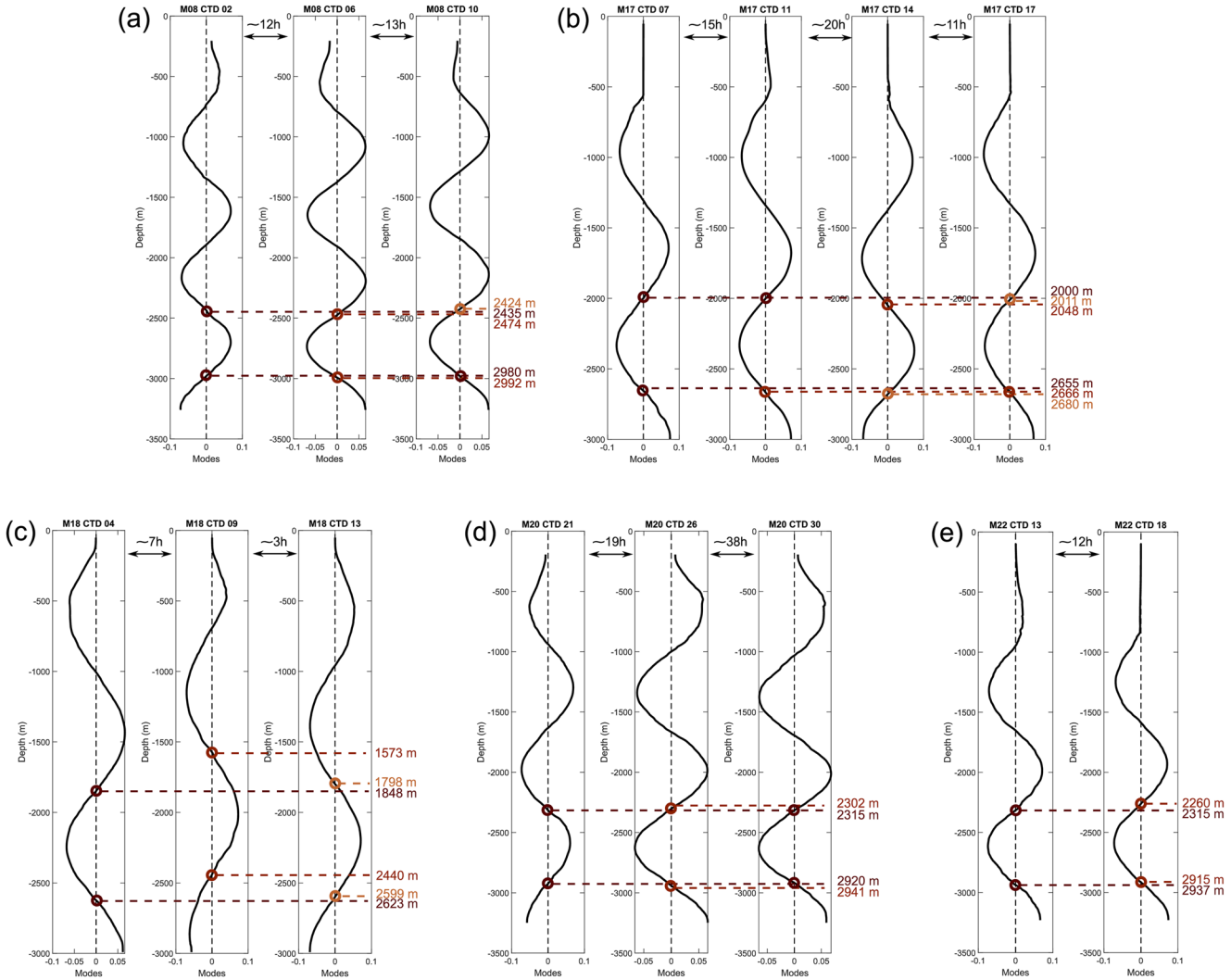

Figure 3. Fifth modes of the normal mode decomposition for the casts performed during (a) December 1999, (b) March 2002, (c) April 2002, (d) August 2002, and (e) July 2003. Circles identify the zero-crossings, and for each of them are reported the corresponding equivalent depths. Black dashed lines indicate the zero line. Between the panels is reported approximately the time span between one cast and another of the same acquisition campaign.

variances were obtained by integrating over rolling segments of 320 m to account for non-homogeneity in the statistical distribution of the water column properties and to have a more robust representation of the fine-scale variability. Integration has been done in the internal wave range corresponding to wavelengths of 160 and 20 m, ceiling the strain variance to 0.1 if it is above a minimum for the GM integration corresponding to 25 m to avoid saturation, which would lead to overestimated values (A. E. Gargett, 1990; Gregg et al., 2003; Kunze et al., 2006; Pollmann, 2020).

3. Results and Discussion

The seasonal variability of the Ionian Sea heavily affects circulation patterns at the surface and intermediate layers, with stronger winter flows (Millot & Taupier-Letage, 2005; Pinardi et al., 2015; Robinson et al., 1991). This seasonal variability can be recognized in the temperature and salinity profiles in Figures 2a and 2b, despite the casts being performed from 50 to 100 m above the surface. CTD profiles include all seasons, with M08 and M17 having a similar behavior, corresponding to winter periods with colder mean temperature values ($\Theta \sim 13.9$°C) and saltier mean salinity values ($S_A \sim 38.98$ g kg^{-1}) in the upper 500 m. In contrast, M18, measured at the end of April, has higher mean temperatures ($\Theta \sim 14.3$°C) and lower mean salinity values ($S_A \sim 38.96$ g kg^{-1}) in the

upper 500 m, consistent with the sea surface temperature observations of the period. M20 and M22, measured late in summer, have similar values among them and, in general, are similar to the other profiles since both of them were sampled starting from 100 m and below, but they show a high variability at intermediate depths. The LIW can be identified in the Absolute Salinity-Conservative Temperature ($S_A - \theta$) diagram for the shallower casts (Figure 2c). The deeper layers have a small seasonal variation and are occupied by the EMDW, below the LIW until 2,000 m depth, where there is a smaller peak in the diagram that we identified as Ionian Abyssal Water (IAW) between 2,000 and 3,000 m to the bottom (Figure 2c). The introduction of IAW is meant to account for the significant change in the thermohaline structure in the deepest layer over 5 years (Figure 2). This is in accordance with the observed adjustment of the area to the EMT: the Ionian abyssal layer state was perturbed by the entrainment of Cretan Deep Water (CDW), which formed a thick homogeneous layer of warmer and saltier waters that stabilized between 2003 and 2011 (Artale et al., 2018; Bensi et al., 2013; Manca et al., 2006; Rubino et al., 2016). In the EMT-induced stratification both EMDW and CDW are competing as bottom water sources for the Ionian basin, and the differences among them are complex to classify (Rubino et al., 2016).

We investigate the effects of the presence of the IAW in the behavior of the water column through the fifth mode of oscillation of the normal mode decomposition (Figure 3). The three M08 casts (Figure 3a) were measured ∼12 hr apart from each other and show little variations of the zero-crossing depths, of the order of 10 m, which correspond to the uncertainty on the mode calculation. The four M17 casts (Figure 3b) were taken at different time spans. The zero-crossings of the profiles with a time span larger than 11 hr remain almost at the same level, while the last two casts have a zero-crossing difference with the previous casts of a tenth meter. The cast CTD 14 and CTD 17 of M17 have a zero-crossing difference between them of ∼14 m for the equivalent depth of ∼2,600 m, and ∼38 m for the equivalent depth of ∼2,000 m. The three M18 casts (Figure 3c) show an evident oscillation in the deep layer, with ∼183 m of variation for the equivalent depth of ∼2,500 m, and ∼275 m for the equivalent depth of ∼1,700 m. These were the casts measured within the smallest time span. The three M20 casts (Figure 3d) were measured ∼19 and ∼38 hr apart respectively, and show little zero-crossing variations, of the order of 10 m. The two M22 casts (Figure 3e) were measured after ∼12 hr from one another. The deepest zero-crossing, at an equivalent depth of ∼2,900 m, goes up ∼22 m, and the above zero-crossing, corresponding to an equivalent depth of ∼2,250, goes up ∼55 m. Therefore, what can be observed in Figure 3 is that the deepest zero-crossings of casts with a time span between one another smaller than ∼12 hr have a periodic variation that is not present when a long time has passed.

To further investigate the observed tidal-period oscillation of the deep layers in the M18 casts (Figure 3c) we reconstructed the isopycnal variability and estimated the diffusivity coefficient. From the potential density profiles at 1,500–3,000 m of depth (Figure 4a) we can identify a temporal sequence of density overturns, significantly, in the second profile (M18 CTD 09). The diffusivities associated with the overturns show a peak near and above $10^{-5}(m^2\,s^{-1})$, which is within the common observations and the expected values to sustain diapycnal circulation (Munk, 1966; Munk & Wunsch, 1998). The sorted M18 profiles (Figure 4a) are useful to identify instabilities and consequently significant density differences in the original profile (A. Gargett & Garner, 2008). This allowed highlighting the time variations: the third profile (M18 CTD 13) tends to realign with the first one (M18 CTD 04), while the second one (M18 CTD 09) departs from this behavior at ∼2,000–2,350 m, confirming that the profile catches isopycnals moving at that time under the tidal period (dotted lines in Figure 4a). This signal can be interpreted as a pre-condition of overturning, which would be confirmed by velocity field information, unluckily not available for this area. The presence of a high-density zone under 2,500 m in the second profile indicates that something must have lifted it up. Since the profiling location is 71.8 km from the Malta Escarpment (Figure 1), this should be due to bathymetry interaction with internal tides generated on the steep Escarpment, guided by the well-defined stratification of the deep layers (Ferrari et al., 2016). We exclude locally other mesoscale processes because the time scales needed for composite perturbation patterns generally range from a few days to a few weeks (Rubino et al., 2012), and the M18 profiles were acquired over 12 hr, which is above the near-inertial frequency peak observed in the area which is ∼17 hr (Giambenedetti et al., 2023).

To sustain our reasoning on the time dependence of the oscillation, we evaluated the diffusion coefficient (Equation 3) using a time-averaged $\overline{N^2}$ profile for the strain calculation in Equation 4 (Figure 4b). Nearby the IAW heights K_{iw} has values of $O(10^{-5})$, greater than the background turbulence generally observed, and consistent with the baroclinic tidal influence which is a second-order effect with respect to the local dynamics. This suggests an activation of mixing in the M18 CTD 09 profile, with K_{iw} values not extremely far from the GM reference values, validating all the analyses made so far. The K_{iw} values estimated without applying

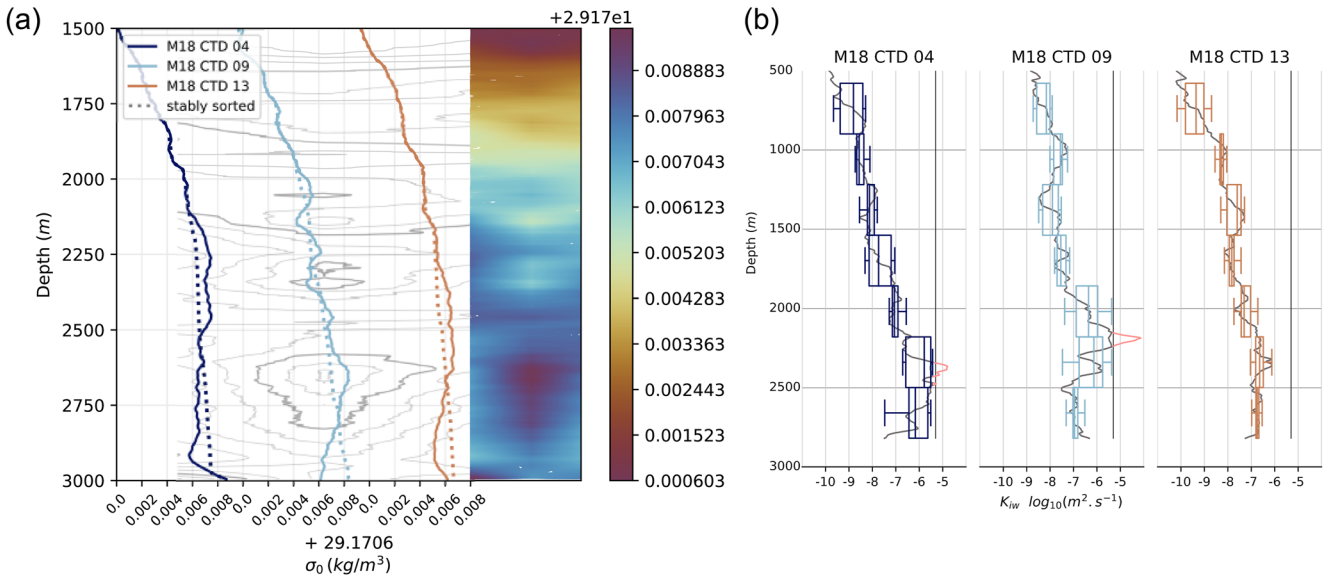

Figure 4. (a) Vertical profiles of potential density (σ_0): dashed lines are the sorted profiles, gray curves and colored right panel show the contours of isopycnal levels; (b) diffusion coefficient (K_{iw}) evaluated for the M18 profiles, with boxplots performed on 320 m separated z-segments showing the uncertainty associated with the choice of segment lengths and position. Solid black line indicates the GM value, and in red is shown the K_{iw} estimation without the saturation criteria. Colormap by Crameri (Crameri, 2018).

the saturation criteria were overestimated in depth (red line in Figure 4b): the energy transfer at fine-scale activates before GM in observed strain variance spectra, and to evaluate the behavior correctly with respect to the model is necessary to put a condition on the total amount of energy available (A. E. Gargett, 1990; Pollmann, 2020).

This diffusivity enhancement in the abyssal layer, combined with the tidal periodicity, clearly indicates that the observed perturbation is the consequence of a baroclinic tide wave breaking on the near Malta Escarpment. Its impact on activating energy exchange/mixing is therefore non-negligible when integrated over time in energy budgets, having direct consequences on the redistribution of heat and tracers in the water column.

4. Conclusions

The concurrence of several factors, that is, the unusual sampling method used for the CTD casts, the presence of a dense deep water mass (the IAW), and the multi-method approach, made it possible to undoubtedly identify a tidal-period variability in the deepest layer of the water column and the consequent activation of mixing at finer scales.

Tidal influence at 3,000 m of depth is not so straightforward to observe as well as inertial signals, and what we found is that it has a non-negligible role in the vertical transport of energy. To date, there are still few direct observations of deep mixing. However, by combining different indirect methodologies we can get a realistic representation of what happens at depths, even at smaller scales, exploiting the existing resources at best. These observations are consistent with the generally accepted idea that energy redistribution through morphology interaction requires tidal processes to explain the observed dissipation rates (MacKinnon et al., 2017; Meredith & Garbato, 2021; Wunsch & Ferrari, 2004), meaning that it is a process that has a non-negligible role even in the Mediterranean Sea, where tides amplitude is way less than in the global oceans (Cushman-Roisin & Naimie, 2002; Millot & Taupier-Letage, 2005).

Our results can be useful for driving future research in the Mediterranean region, pointing out that deep stratification and tidal forcing should be included in the numerical simulations, and that there is a need for exploring areas where their effect is greater, by performing continuous and more comprehensive measurements.

Finally, our analysis demonstrated that the application of multiple methodologies an ad hoc in situ measurements, collected under process-based hypotheses, is a successful approach to exploit limited data availability.

Conflict of Interest

The authors declare no conflicts of interest relevant to this study.

Data Availability Statement

Original raw data were provided by Giorgio Riccobene and Antonio Capone. The CTD profiles were conducted between 1999 and 2003 in the framework of the Cubic Kilometer Neutrino Telescope (KM3NeT) project (Adrián-Martínez et al., 2016; Katz, 2006; Migneco et al., 2008; Riccobene et al., 2007; Rubino et al., 2012). Specifically, they were acquired during EMTEC cruises (April–May 1999), SINAPSI-4 cruise (March–April 2002), Poseidon Cruise 298 (May 2003). The processed datasets used for this study are available via doi.org/10.5281/zenodo.7871735.

Acknowledgments
Open Access Funding provided by Istituto Nazionale di Geofisica e Vulcanologia (INGV) within the CRUI-CARE Agreement.

References

Adrián-Martínez, S., Ageron, M., Aharonian, F., Aiello, S., Albert, A., Ameli, F., et al. (2016). Letter of intent for KM3NeT 2.0. *Journal of Physics G: Nuclear and Particle Physics*, *43*(8), 084001. https://doi.org/10.1088/0954-3899/43/8/084001

Alford, M. H. (2003). Redistribution of energy available for ocean mixing by long-range propagation of internal waves. *Nature*, *423*(6936), 159–162. https://doi.org/10.1038/nature01628

Arbic, B. K. (2022). Incorporating tides and internal gravity waves within global ocean general circulation models: A review. *Progress in Oceanography*, *206*, 102824. https://doi.org/10.1016/j.pocean.2022.102824

Arbic, B. K., Alford, M. H., Ansong, J. K., Buijsman, M. C., Ciotti, R. B., Farrar, J. T., et al. (2018). A primer on global internal tide and internal gravity wave continuum modeling in HYCOM and MITgcm. In E. Chassignet, A. Pascual, J. Tintore, & J. Verron (Eds.), *New frontiers in operational oceanography* (pp. 307–392). GODAE OceanView. https://doi.org/10.17125/gov2018.ch13

Artale, V., Falcini, F., Marullo, S., Bensi, M., Kokoszka, F., Iudicone, D., & Rubino, A. (2018). Linking mixing processes and climate variability to the heat content distribution of the Eastern Mediterranean abyss. *Scientific Reports*, *8*(1), 11317. https://doi.org/10.1038/s41598-018-29343-4

Artale, V., Levi, D., Marullo, S., & Santoleri, R. (1990). Analysis of nonlinear internal waves observed by Landsat thematic mapper. *Journal of Geophysical Research*, *95*(C9), 16065. https://doi.org/10.1029/JC095iC09p16065

Astraldi, M., Gasparini, G. P., Vetrano, A., & Vignudelli, S. (2002). Hydrographic characteristics and interannual variability of water masses in the central Mediterranean: A sensitivity test for long-term changes in the Mediterranean Sea. *Deep Sea Research Part I: Oceanographic Research Papers*, *49*(4), 661–680. https://doi.org/10.1016/S0967-0637(01)00059-0

Bensi, M., Rubino, A., Cardin, V., Hainbucher, D., & Mancero-Mosquera, I. (2013). Structure and variability of the abyssal water masses in the Ionian Sea in the period 2003-2010: Ionian Sea abyssal changes. *Journal of Geophysical Research: Oceans*, *118*(2), 931–943. https://doi.org/10.1029/2012JC008178

Bensi, M., Velaoras, D., Meccia, V. L., & Cardin, V. (2016). Effects of the Eastern Mediterranean Sea circulation on the thermohaline properties as recorded by fixed deep-ocean observatories. *Deep Sea Research Part I: Oceanographic Research Papers*, *112*, 1–13. https://doi.org/10.1016/j.dsr.2016.02.015

Budillon, G., Bue, N. L., Siena, G., & Spezie, G. (2010). Hydrographic characteristics of water masses and circulation in the Northern Ionian Sea. *Deep Sea Research Part II: Topical Studies in Oceanography*, *57*(5–6), 441–457. https://doi.org/10.1016/j.dsr2.2009.08.017

Bushnell, M., Waldmann, C., Seitz, S., Buckley, E., Tamburri, M., Hermes, J., et al. (2019). Quality assurance of oceanographic observations: Standards and guidance adopted by an international partnership. *Frontiers in Marine Science*, *6*, 706. https://doi.org/10.3389/fmars.2019.00706

Cao, A.-Z., Li, B.-T., & Lv, X.-Q. (2015). Extraction of internal tidal currents and reconstruction of full-depth tidal currents from mooring observations. *Journal of Atmospheric and Oceanic Technology*, *32*(7), 1414–1424. https://doi.org/10.1175/JTECH-D-14-00221.1

Cavaliere, D., la Forgia, G., Adduce, C., Alpers, W., Martorelli, E., & Falcini, F. (2021). Breaking location of internal solitary waves over a sloping seabed. *Journal of Geophysical Research: Oceans*, *126*, e2020JC016669. https://doi.org/10.1029/2020JC016669

Crameri, F. (2018). Scientific colour maps. *Zenodo*. https://doi.org/10.5281/zenodo.1243862

Cushman-Roisin, B., & Naimie, C. E. (2002). A 3D finite-element model of the Adriatic tides. *Journal of Marine Systems*, *37*(4), 279–297. https://doi.org/10.1016/S0924-7963(02)00204-X

De Lavergne, C., Groeskamp, S., Zika, J., & Johnson, H. L. (2022). The role of mixing in the large-scale ocean circulation. *Ocean Mixing*, 35–63. https://doi.org/10.1016/B978-0-12-821512-8.00010-4

Ferrari, R., Mashayek, A., Mcdougall, T. J., Nikurashin, M., & Campin, J.-M. (2016). Turning ocean mixing upside down. *Journal of Physical Oceanography*, *46*(7), 2239–2261. https://doi.org/10.1175/jpo-d-15-0244.1

Fox-Kemper, B. (2021). Ocean, cryosphere and sea level change. In *AGU fall meeting abstracts, 2021, U13B-09*.

Gargett, A., & Garner, T. (2008). Determining thorpe scales from ship-lowered CTD density profiles. *Journal of Atmospheric and Oceanic Technology*, *25*(9), 1657–1670. https://doi.org/10.1175/2008JTECHO541.1

Gargett, A. E. (1990). Do we really know how to scale the turbulent kinetic energy dissipation rate ε due to breaking of oceanic internal waves? *Journal of Geophysical Research*, *95*(C9), 15971. https://doi.org/10.1029/JC095iC09p15971

Garrett, C., & Munk, W. (1979). Internal waves in the ocean. *Annual Review of Fluid Mechanics*, *11*(1), 339–369. https://doi.org/10.1146/annurev.fl.11.010179.002011

Giambenedetti, B., Bue, N. L., Artale, V., & Falcini, F. (2023). Role of stratification in vorticity propagation throughout the entire water column: A Mediterranean example (Ionian Sea) (No. EGU23-13857). In *EGU23. Copernicus meetings*. https://doi.org/10.5194/egusphere-egu23-13857

Gill, A. E. (1982). *Atmosphere-ocean dynamics (Nachdr.)*. Acad. Press.

Glover, A. G., Gooday, A. J., Bailey, D. M., Billett, D. S. M., Chevaldonné, P., Colaço, A., et al. (2010). Temporal change in deep-sea benthic ecosystems. In *Advances in marine biology* (Vol. 58, pp. 1–95). Elsevier. https://doi.org/10.1016/B978-0-12-381015-1.00001-0

Gregg, M. C., Sanford, T. B., & Winkel, D. P. (2003). Reduced mixing from the breaking of internal waves in equatorial waters. *Nature*, *422*(6931), 513–515. https://doi.org/10.1038/nature01507

Griffiths, S. D., & Grimshaw, R. H. J. (2007). Internal tide generation at the continental shelf modeled using a modal decomposition: Two-dimensional results. *Journal of Physical Oceanography*, *37*(3), 428–451. https://doi.org/10.1175/JPO3068.1

Hainbucher, D., Rubino, A., & Klein, B. (2006). Water mass characteristics in the deep layers of the western Ionian Basin observed during May 2003. *Geophysical Research Letters*, *33*(5), L05608. https://doi.org/10.1029/2005GL025318

Incarbona, A., Martrat, B., Mortyn, P. G., Sprovieri, M., Ziveri, P., Gogou, A., et al. (2016). Mediterranean circulation perturbations over the last five centuries: Relevance to past Eastern Mediterranean Transient-type events. *Scientific Reports*, *6*(1), 29623. https://doi.org/10.1038/srep29623

IOC, SCOR, & IAPSO. (2010). The international thermodynamic equation of seawater – 2010: Calculation and use of thermodynamic properties. *Intergovernmental Oceanographic Commission, Manuals and Guides*, *56*, 196.

Katz, U. F. (2006). KM3NeT: Towards a km3 Mediterranean neutrino telescope. *Nuclear Instruments and Methods in Physics Research Section A: Accelerators, Spectrometers, Detectors and Associated Equipment*, *567*(2), 457–461. https://doi.org/10.1016/j.nima.2006.05.235

Klein, B., Roether, W., Manca, B. B., Bregant, D., Beitzel, V., Kovacevic, V., & Luchetta, A. (1999). The large deep water transient in the Eastern Mediterranean. *Deep Sea Research Part I: Oceanographic Research Papers*, *46*(3), 371–414. https://doi.org/10.1016/S0967-0637(98)00075-2

Klocker, A., & McDougall, T. J. (2010). Influence of the nonlinear equation of state on global estimates of dianeutral advection and diffusion. *Journal of Physical Oceanography*, *40*(8), 1690–1709. https://doi.org/10.1175/2010JPO4303.1

Koseff, J. R., Woodson, C. B., Pawlak, G., & Monismith, S. G. (2016). Direct measurements of flux Richardson number in the nearshore coastal ocean. In *VIIIth Int. Symp. on stratified flows, San Diego*.

Kunze, E., Firing, E., Hummon, J. M., Chereskin, T. K., & Thurnherr, A. M. (2006). Global abyssal mixing inferred from lowered ADCP shear and CTD strain profiles. *Journal of Physical Oceanography*, *36*(8), 1553–1576. https://doi.org/10.1175/JPO2926.1

Kunze, E., MacKay, C., McPhee-Shaw, E. E., Morrice, K., Girton, J. B., & Terker, S. R. (2012). Turbulent mixing and exchange with interior waters on sloping boundaries. *Journal of Physical Oceanography*, *42*(6), 910–927. https://doi.org/10.1175/JPO-D-11-075.1

LeBlond, P. H., & Mysak, L. A. (1978). *Waves in the ocean*. Elsevier.

Levin, L. A., Bett, B. J., Gates, A. R., Heimbach, P., Howe, B. M., Janssen, F., et al. (2019). Global observing needs in the deep ocean. *Frontiers in Marine Science*, *6*, 241. https://doi.org/10.3389/fmars.2019.00241

Li, P., & Tanhua, T. (2020). Recent changes in deep ventilation of the Mediterranean Sea; Evidence from long-term transient tracer observations. *Frontiers in Marine Science*, *7*, 594. https://doi.org/10.3389/fmars.2020.00594

Li, Z., von Storch, J. S., & Müller, M. (2015). The M2 internal tide simulated by a 1/10∘ OGCM. *Journal of Physical Oceanography*, *45*(12), 3119–3135. https://doi.org/10.1175/JPO-D-14-0228.1

MacKinnon, J. A., Zhao, Z., Whalen, C. B., Waterhouse, A. F., Trossman, D. S., Sun, O. M., et al. (2017). Climate process team on internal wave–driven ocean mixing. *Bulletin of the American Meteorological Society*, *98*(11), 2429–2454. https://doi.org/10.1175/BAMS-D-16-0030.1

Makris, J., & Stobbe, C. (1984). Physical properties and state of the crust and upper mantle of the Eastern Mediterranean Sea deduced from geophysical data. *Marine Geology*, *55*(3–4), 347–363. https://doi.org/10.1016/0025-3227(84)90076-8

Manca, B. (2003). Evolution of dynamics in the eastern Mediterranean affecting water mass structures and properties in the Ionian and Adriatic Seas. *Journal of Geophysical Research*, *108*(C9), 8102. https://doi.org/10.1029/2002JC001664

Manca, B., Ibello, V., Pacciaroni, M., Scarazzato, P., & Giorgetti, A. (2006). Ventilation of deep waters in the Adriatic and Ionian Seas following changes in thermohaline circulation of the Eastern Mediterranean. *Climate Research*, *31*, 239–256. https://doi.org/10.3354/cr031239

Meredith, M., & Garbato, A. (2021). *Ocean mixing—Drivers, mechanisms, and impacts*. Elsevier. Retrieved from https://www.elsevier.com/books/ocean-mixing/meredith/978-0-12-821512-8

Migneco, E., Aiello, S., Aloisio, A., Ameli, F., Amore, I., Anghinolfi, M., et al. (2008). Recent achievements of the NEMO project. *Nuclear Instruments and Methods in Physics Research Section A: Accelerators, Spectrometers, Detectors and Associated Equipment*, *588*(1–2), 111–118. https://doi.org/10.1016/j.nima.2008.01.012

Millot, C., & Taupier-Letage, I. (2005). Circulation in the Mediterranean Sea. In A. Saliot (Ed.), *The Mediterranean Sea* (Vol. 5K, pp. 29–66). Springer Berlin Heidelberg. https://doi.org/10.1007/b107143

Müller, M., Cherniawsky, J., Foreman, M., & von Storch, J.-S. (2012). Global map of M2 internal tide and its seasonal variability from high resolution ocean circulation and tide modelling. *Geophysical Research Letters*, *39*(19), L19607. https://doi.org/10.1029/2012GL053320

Munk, W. (1966). Abyssal recipes. *Deep Sea Research and Oceanographic Abstracts*, *13*(4), 707–730. https://doi.org/10.1016/0011-7471(66)90602-4

Munk, W., & Wunsch, C. (1998). Abyssal recipes II: Energetics of tidal and wind mixing. *Deep Sea Research Part I: Oceanographic Research Papers*, *45*(12), 1977–2010. https://doi.org/10.1016/S0967-0637(98)00070-3

Nakano, H., & Yoshida, J. (2019). A note on estimating eddy diffusivity for oceanic double-diffusive convection. *Journal of Oceanography*, *75*(5), 375–393. https://doi.org/10.1007/s10872-019-00514-9

Nash, K. L., Alexander, K., Melbourne-Thomas, J., Novaglio, C., Sbrocchi, C., Villanueva, C., & Pecl, G. T. (2022). Developing achievable alternate futures for key challenges during the UN decade of ocean science for sustainable development. *Reviews in Fish Biology and Fisheries*, *32*(1), 19–36. https://doi.org/10.1007/s11160-020-09629-5

Oakey, N. S. (1982). Determination of the rate of dissipation of turbulent energy from simultaneous temperature and velocity shear microstructure measurements. *Journal of Physical Oceanography*, *12*(3), 256–271. https://doi.org/10.1175/1520-0485(1982)012<0256:dotrod>2.0.co;2

Osborn, T. R. (1980). Estimates of the local rate of vertical diffusion from dissipation measurements. *Journal of Physical Oceanography*, *10*(1), 83–89. https://doi.org/10.1175/1520-0485(1980)010<0083:eotlro>2.0.co;2

Osborn, T. R., & Cox, C. S. (1972). Oceanic fine structure. *Geophysical Fluid Dynamics*, *3*(4), 321–345. https://doi.org/10.1080/03091927208236085

Pauthenet, E., Roquet, F., Madec, G., Sallée, J.-B., & Nerini, D. (2019). The thermohaline modes of the global ocean. *Journal of Physical Oceanography*, *49*(10), 2535–2552. https://doi.org/10.1175/JPO-D-19-0120.1

Pedlosky, J. (1996). *Ocean circulation theory*. Springer Berlin Heidelberg. https://doi.org/10.1007/978-3-662-03204-6

Pinardi, N., Zavatarelli, M., Adani, M., Coppini, G., Fratianni, C., Oddo, P., et al. (2015). Mediterranean Sea large-scale low-frequency ocean variability and water mass formation rates from 1987 to 2007: A retrospective analysis. *Progress in Oceanography*, *132*, 318–332. https://doi.org/10.1016/j.pocean.2013.11.003

Polejack, A. (2021). The importance of Ocean Science diplomacy for ocean affairs, global sustainability, and the UN decade of ocean science. *Frontiers in Marine Science*, *8*, 664066. https://doi.org/10.3389/fmars.2021.664066

Pollmann, F. (2020). Global characterization of the ocean's internal wave spectrum. *Journal of Physical Oceanography*, *50*(7), 1871–1891. https://doi.org/10.1175/JPO-D-19-0185.1

Polzin, K. L., Toole, J. M., Ledwell, J. R., & Schmitt, R. W. (1997). Spatial variability of turbulent mixing in the abyssal ocean. *Science*, *276*(5309), 93–96. https://doi.org/10.1126/science.276.5309.93

Riccobene, G., Capone, A., Aiello, S., Ambriola, M., Ameli, F., Amore, I., et al. (2007). Deep seawater inherent optical properties in the Southern Ionian Sea. *Astroparticle Physics*, *27*(1), 1–9. https://doi.org/10.1016/j.astropartphys.2006.08.006

Robinson, A. R., Golnaraghi, M., Leslie, W. G., Artegiani, A., Hecht, A., Lazzoni, E., et al. (1991). The eastern Mediterranean general circulation: Features, structure and variability. *Dynamics of Atmospheres and Oceans*, *15*(3–5), 215–240. https://doi.org/10.1016/0377-0265(91)90021-7

Roether, W., Manca, B. B., Klein, B., Bregant, D., Georgopoulos, D., Beitzel, V., et al. (1996). Recent changes in Eastern Mediterranean deep waters. *Science*, *271*(5247), 333–335. https://doi.org/10.1126/science.271.5247.333

Rubino, A., Androssov, A., & Dotsenko, S. (2007). Intrinsic dynamics and long-term evolution of a convectively generated oceanic vortex in the Greenland Sea. *Geophysical Research Letters*, *34*, L16607. https://doi.org/10.1029/2007GL030634

Rubino, A., Bensi, M., Hainbucher, D., Zanchettin, D., Mapelli, F., Ogrinc, N., et al. (2016). Biogeochemical, isotopic and bacterial distributions trace oceanic abyssal circulation. *PLoS One*, *11*(1), e0145299. https://doi.org/10.1371/journal.pone.0145299

Rubino, A., Falcini, F., Zanchettin, D., Bouche, V., Salusti, E., Bensi, M., et al. (2012). Abyssal undular vortices in the Eastern Mediterranean basin. *Nature Communications*, *3*(1), 834. https://doi.org/10.1038/ncomms1836

Ruhl, H. A., André, M., Beranzoli, L., Çağatay, M. N., Colaço, A., Cannat, M., et al. (2011). Societal need for improved understanding of climate change, anthropogenic impacts, and geo-hazard warning drive development of ocean observatories in European Seas. *Progress in Oceanography*, *91*(1), 1–33. https://doi.org/10.1016/j.pocean.2011.05.001

Sannino, G., Carillo, A., Iacono, R., Napolitano, E., Palma, M., Pisacane, G., & Struglia, M. (2022). Modelling present and future climate in the Mediterranean Sea: A focus on sea-level change. *Climate Dynamics*, *59*(1–2), 357–391. https://doi.org/10.1007/s00382-021-06132-w

Sannino, G., Carillo, A., Pisacane, G., & Naranjo, C. (2015). On the relevance of tidal forcing in modelling the Mediterranean thermohaline circulation. *Progress in Oceanography*, *134*, 304–329. https://doi.org/10.1016/j.pocean.2015.03.002

Simmons, H. L., Hallberg, R. W., & Arbic, B. K. (2004). Internal wave generation in a global baroclinic tide model. *Deep Sea Research Part II: Topical Studies in Oceanography*, *51*(25–26), 3043–3068. https://doi.org/10.1016/j.dsr2.2004.09.015

Stammer, D., Bracco, A., Braconnot, P., Brasseur, G. P., Griffies, S. M., & Hawkins, E. (2018). Science directions in a Post COP21 world of transient climate change: Enabling regional to local predictions in support of reliable climate information. *Earth's Future*, *6*(11), 1498–1507. https://doi.org/10.1029/2018EF000979

St. Laurent, L. C., Toole, J. M., & Schmitt, R. W. (2001). Buoyancy forcing by turbulence above rough topography in the abyssal Brazil Basin. *Journal of Physical Oceanography*, *31*(12), 3476–3495. https://doi.org/10.1175/1520-0485(2001)031<3476:BFBTAR>2.0.CO;2

Theocharis, A., Georgopoulos, D., Lascaratos, A., & Nittis, K. (1993). Water masses and circulation in the central region of the Eastern Mediterranean: Eastern Ionian, South Aegean and Northwest Levantine, 1986–1987. *Deep Sea Research Part II: Topical Studies in Oceanography*, *40*(6), 1121–1142. https://doi.org/10.1016/0967-0645(93)90064-T

Theocharis, A., Klein, B., Nittis, K., & Roether, W. (2002). Evolution and status of the Eastern Mediterranean transient (1997–1999). *Journal of Marine Systems*, *33*, 91–116. https://doi.org/10.1016/S0924-7963(02)00054-4

Tintoré, J., Pinardi, N., Álvarez-Fanjul, E., Aguiar, E., Álvarez-Berastegui, D., Bajo, M., et al. (2019). Challenges for sustained observing and forecasting systems in the Mediterranean Sea. *Frontiers in Marine Science*, *6*, 568. https://doi.org/10.3389/fmars.2019.00568

Toole, J. M., Schmitt, R. W., & Polzin, K. L. (1994). Estimates of diapycnal mixing in the abyssal ocean. *Science*, *264*(5162), 1120–1123. https://doi.org/10.1126/science.264.5162.1120

Tsimplis, M. N., Proctor, R., & Flather, R. A. (1995). A two-dimensional tidal model for the Mediterranean Sea. *Journal of Geophysical Research*, *100*(C8), 16223. https://doi.org/10.1029/95JC01671

van Haren, H., & Gostiaux, L. (2011). Large internal waves advection in very weakly stratified deep Mediterranean waters: Large waves in deep Mediterranean. *Geophysical Research Letters*, *38*(22), n/a. https://doi.org/10.1029/2011GL049707

Waterhouse, A. F., MacKinnon, J. A., Nash, J. D., Alford, M. A., Kunze, E., Simmons, H. L., et al. (2014). Global patterns of diapycnal mixing from measurements of the turbulent dissipation rate. *Journal of Physical Oceanography*, *44*(7), 1854–1872. https://doi.org/10.1175/JPO-D-13-0104.1

Wüest, A., & Lorke, A. (2003). Small-scale hydrodynamics in lakes. *Annual Review of Fluid Mechanics*, *35*(1), 373–412. https://doi.org/10.1146/annurev.fluid.35.101101.161220

Wüst, G. (1961). On the vertical circulation of the Mediterranean Sea. *Journal of Geophysical Research*, *66*(10), 3261–3271. https://doi.org/10.1029/JZ066i010p03261

Wunsch, C., & Ferrari, R. (2004). Vertical mixing, energy, and the general circulation of the oceans. *Annual Review of Fluid Mechanics*, *36*(1), 281–314. https://doi.org/10.1146/annurev.fluid.36.050802.122121